Genotypic and Phenotypic Spectrum of Foveal Hypoplasia

A Multicenter Study

Helen J. Kuht, BMedSci, PhD,[1,28] Gail D.E. Maconachie, BMedSci, PhD,[1,2,28] Jinu Han, MD,[3,28]
Line Kessel, MD, PhD,[4,5,28] Maria M. van Genderen, MD, PhD,[6,7,28] Rebecca J. McLean, MSc, PhD,[1]
Michael Hisaund, BMedSci,[1] Zhanhan Tu, MBChB, PhD,[1,28] Richard W. Hertle, MD,[8,28]
Karen Gronskov, PhD,[9,28] Dayong Bai, MD, PhD,[10,28] Aihua Wei, MD, PhD,[11,28] Wei Li, PhD,[12,28]
Yonghong Jiao, MD,[13,28] Vasily Smirnov, MD,[14,28] Jae-Hwan Choi, MD,[15,28] Martin D. Tobin, MD,[16,28]
Viral Sheth, BMedSci, PhD,[1,2] Ravi Purohit, BMedSci, PhD,[1] Basu Dawar, MBChB,[1]
Ayesha Girach, MBChB, MSc,[1] Sasha Strul, MD,[17,28] Laura May, CO,[17,28] Fred K. Chen, PhD, FRANZCO,[18,28]
Rachael C. Heath Jeffery, MChD, MPH,[18,28] Abdullah Aamir, MBChB,[1] Ronaldo Sano, PhD, MD,[19,28]
Jing Jin, MD,[20,30] Brian P. Brooks, MD, PhD,[21,28] Susanne Kohl, PhD,[22,28] Benoit Arveiler, PhD,[23,28]
Lluis Montoliu, PhD,[24,28] Elizabeth C. Engle, MD,[25,26,28] Frank A. Proudlock, PhD,[1] Garima Nishad,[27]
Prateek Pani,[27] Girish Varma, PhD,[27,28] Irene Gottlob, MD, FRCOphth,[1,28,29]
Mervyn G. Thomas, PhD, FRCOphth[1,28]

Purpose: To characterize the genotypic and phenotypic spectrum of foveal hypoplasia (FH).

Design: Multicenter, observational study.

Participants: A total of 907 patients with a confirmed molecular diagnosis of albinism, *PAX6*, *SLC38A8*, *FRMD7*, *AHR*, or achromatopsia from 12 centers in 9 countries (n = 523) or extracted from publicly available datasets from previously reported literature (n = 384).

Methods: Individuals with a confirmed molecular diagnosis and availability of foveal OCT scans were identified from 12 centers or from the literature between January 2011 and March 2021. A genetic diagnosis was confirmed by sequence analysis. Grading of FH was derived from OCT scans.

Main Outcome Measures: Grade of FH, presence or absence of photoreceptor specialization (PRS+ vs. PRS−), molecular diagnosis, and visual acuity (VA).

Results: The most common genetic etiology for typical FH in our cohort was albinism (67.5%), followed by *PAX6* (21.8%), *SLC38A8* (6.8%), and *FRMD7* (3.5%) variants. *AHR* variants were rare (0.4%). Atypical FH was seen in 67.4% of achromatopsia cases. Atypical FH in achromatopsia had significantly worse VA than typical FH ($P < 0.0001$). There was a significant difference in the spectrum of FH grades based on the molecular diagnosis (chi-square = 60.4, $P < 0.0001$). All *SLC38A8* cases were PRS− ($P = 0.003$), whereas all *FRMD7* cases were PRS+ ($P < 0.0001$). Analysis of albinism subtypes revealed a significant difference in the grade of FH (chi-square = 31.4, $P < 0.0001$) and VA ($P = 0.0003$) between oculocutaneous albinism (OCA) compared with ocular albinism (OA) and Hermansky−Pudlak syndrome (HPS). Ocular albinism and HPS demonstrated higher grades of FH and worse VA than OCA. There was a significant difference ($P < 0.0001$) in VA between *FRMD7* variants compared with other diagnoses associated with FH.

Conclusions: We characterized the phenotypic and genotypic spectrum of FH. Atypical FH is associated with a worse prognosis than all other forms of FH. In typical FH, our data suggest that arrested retinal development occurs earlier in *SLC38A8*, *OA*, *HPS*, and *AHR* variants and later in *FRMD7* variants. The defined time period of foveal developmental arrest for OCA and *PAX6* variants seems to demonstrate more variability. Our findings provide mechanistic insight into disorders associated with FH and have significant prognostic and diagnostic value. *Ophthalmology 2022;129:708-718 © 2022 by the American Academy of Ophthalmology. This is an open access article under the CC BY license (http://creativecommons.org/licenses/by/4.0/).*

Supplemental material available at www.aaojournal.org.

The normal foveal anatomy consists of the extrusion of the plexiform layers, a formed foveal pit, cone photoreceptor outer segment (OS) lengthening, and outer nuclear layer (ONL) widening relative to the parafoveal OS and ONL.[1] Foveal development begins with the centrifugal displacement of the inner retinal layers, followed by the centripetal migration of the cone photoreceptors toward the incipient fovea and finally cone photoreceptor specialization (PRS) (Fig 1A−E).[2-4] Foveal pit formation begins midgestation and continues postnatally characterized by pit deepening and widening. Simultaneously, outer retinal specialization occurs at a rapid rate in the first 2 years of life, but ONL widening continues up to the age of 13 years.[4] Lengthening of the OS layer represents cone PRS and reflects peak cone photoreceptor density.[5] The maturation of the human fovea is a complex process and is critical for visual function.[4] Many genes are involved in the development of the retina. Pathogenic variants in these genes often cause disruption to the foveal developmental process, resulting in foveal hypoplasia (FH), which describes the underdevelopment of the fovea.[1]

Foveal hypoplasia is characterized by the continuation of inner retinal layers posterior to the foveola, and progressive loss of these foveal elements is represented by increasing grades of FH. Three key foveal development stages form the basis of the Leicester Grading System for FH, developed by Thomas et al[1] (Fig 1F−H). The Leicester Grading System is divided into 4 grades of typical FH (grades 1−4) and 1 grade of atypical FH, which is associated with photoreceptor degeneration.

The Leicester Grading System can be applied to a diverse range of genetic disorders, including albinism, achromatopsia, and those caused by pathogenic variants in *PAX6*, *SLC38A8*, *FRMD7,* and *AHR*. In addition to providing insight into the degree of foveal development, identifying the grade of FH has diagnostic and prognostic implications.[1,7] Rufai et al[7] reported that identifying the grade of FH can predict future visual acuity (VA) in preverbal children with nystagmus.

The introduction of OCT has revolutionized ophthalmic diagnosis with the ability to promptly visualize retinal morphology in a high-resolution, noninvasive manner.[8,9] Furthermore, the advent of handheld OCT has facilitated the foveal examination of pediatric patients.[10] OCT is now available in most ophthalmology clinics and subsequently has rapidly become part of routine ophthalmic assessment.[8] Thus, the necessary technology to identify foveal developmental abnormalities is now accessible in most centers.

The phenotypic spectrum of albinism has been reported, including the variance in degree of arrested retinal development.[11,12] Furthermore, high grades of FH (grades 3 and 4) have recently been consistently associated with *SLC38A8* variants[13]; however, to date, the full spectrum of FH linked with variants of known genes involved in retinal development has not been investigated. Thus, it is unclear whether variants of certain genes known to be related to FH and nystagmus are associated with a more underdeveloped foveal morphology. We performed a comparative study to investigate and characterize the genotypic and phenotypic spectrum of FH in albinism,

achromatopsia, *PAX6*, *SLC38A8*, *FRMD7,* and *AHR* variants.

Methods

In this multicenter study, we collated genotypic and phenotypic data for 907 patients from 12 centers in 9 countries from a cohort of patients with infantile nystagmus or FH over a 10-year period (2011−2021). We set up an international consortium with a special interest in foveal developmental disorders, composed of pediatric ophthalmologists, neuro-ophthalmologists, clinical geneticists, data scientists, and statistical geneticists. Data were collected by our Foveal Development Investigators Group. Inclusion criteria were defined as (1) a molecular diagnosis and (2) report of foveal morphology on OCT. Genes known to be associated with typical FH (Table 1) were selected: *PAX6, SLC38A8, FRMD7, AHR,* and genes underlying both syndromic and nonsyndromic forms of albinism (*TYR, OCA2, TYRP1, SLC45A2, SLC24A5, LRMDA (C10orf11), GPR143, HPS (1−11), LYST*). An overview of the phenotypical characteristics associated with each of these disorders is shown in Table 1. We also included the achromatopsia genes (*CNGB3, CNGA3, GNAT2, PDE6C, PDE6H,* and *ATF6*) associated with atypical FH (Table 1). Previously reported cases that met the inclusion criteria were additionally identified and collected from the literature between 2011 and 2021. We included all patients with foveal morphology documented on OCT and pathogenic variants in any one of the genes listed, irrespective of whether they had FH or normal foveal morphology. This study was approved by the local ethics committee and adhered to the tenets of Declaration of Helsinki.

Grading of Foveal Hypoplasia

Foveal hypoplasia was graded using the Leicester Grading System for FH (Fig 1F, G).[1] Typical FH was diagnosed as grade 1 if OCT revealed incomplete extrusion of the inner retinal layers posterior to the foveola, the presence of a foveal pit (irrespective of depth), lengthening of the OS layer, and widening of the ONL. Foveal hypoplasia was diagnosed as grade 2 if all features of grade 1 were present except there was no longer a foveal pit. Foveal hypoplasia was diagnosed as grade 3 FH if all features of grade 2 FH were present except there was no lengthening of the OS layer. Foveal hypoplasia was diagnosed as grade 4 FH if all features of grade 3 were present except there was no ONL widening (mimicking the appearance of the peripheral retina).[1] Grades 1 and 2 together can be considered to show evidence of cone PRS (PRS+), whereas in grades 3 and 4, there is no evidence of cone PRS (PRS−).[1]

Atypical FH is associated with photoreceptor degeneration and was diagnosed if OCT revealed the disruption of the inner segment ellipsoid associated with continuation of the inner retinal layers posterior to the foveola.[1] Foveal scans were interpreted and graded by experienced clinicians within the Foveal Development Investigators Group.

Multicenter Data Collection

Patients with a confirmed molecular diagnosis and a report of foveal morphology were identified between January 2011 and March 2021 from 12 different sites in 9 countries. Foveal scans were captured with OCT using site-specific protocols previously described (Table S1, available at www.aaojournal.org).[11,13,14] Patient demographic and basic ophthalmic examination findings were included where available. Informed consent was obtained from all involved participants. Ethical approval was received
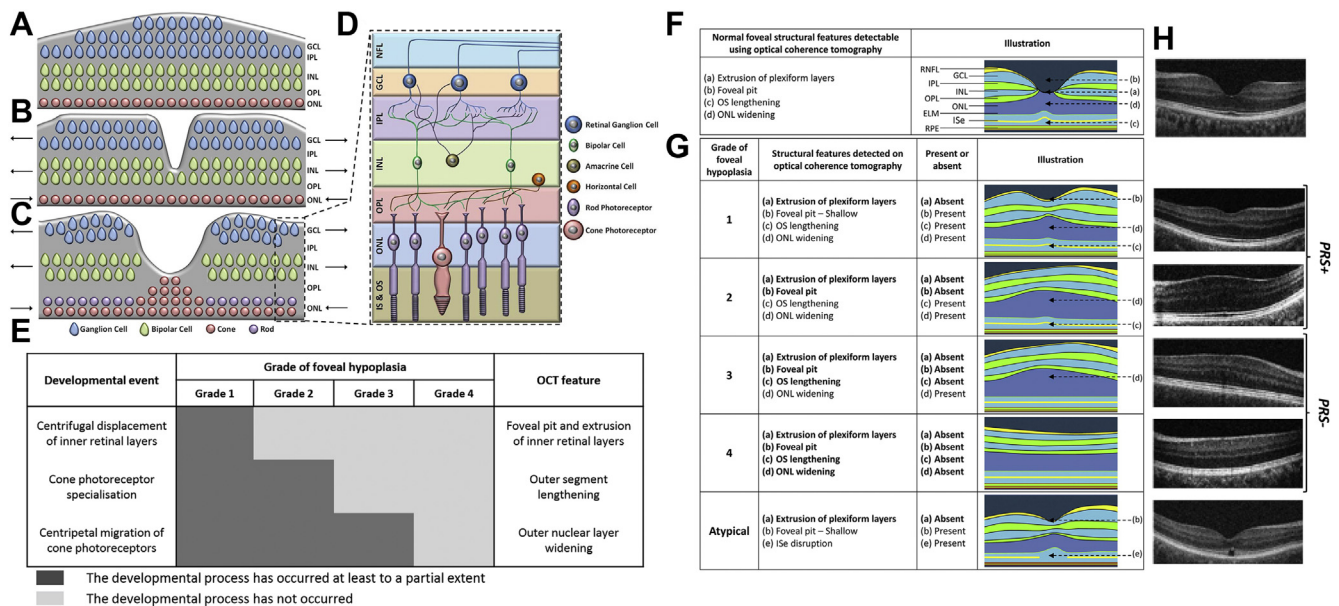
Figure 1. Foveal pit formation and movement of retinal cells during formation of the area of high acuity. **A,** The laminar retinal structure before foveal pit formation. **B,** The inner retinal layers are displaced centrifugally (away from the future fovea) during foveal pit formation. **C,** The cone photoreceptors migrate centripetally (toward the fovea) and form the pure cone area. Arrows point in the direction of movement of the cellular layers. **D,** The magnified laminar structure with the different retinal cell types and the inner segment and outer segment (OS) of the photoreceptors. **A, B,** and **C** are based on developmental theory proposed by Springer and Hendrickson.[6] **E,** Chart showing the 3 developmental processes involved in formation of a structural and functional fovea. In grade 1 foveal hypoplasia (FH), all processes occur to a certain extent; however, in grade 4 FH, none of these processes occur; thus, the retina resembles that of the parafovea. In grades 2 and 3 FH, there is ONL widening but no foveal pit. The difference between grade 2 and 3 FH is occurrence of cone photoreceptor specialization. Identifying these specific features on OCT enables us to understand whether the respective developmental process has occurred. **F,** The unique features of a normal fovea detectable on OCT. **G,** The typical and atypical grades of FH. All grades of FH had incursion of inner retinal layers. Atypical FH also had incursion of the inner retinal layers. Grade 1 FH is associated with a shallow foveal pit, ONL widening, and OS lengthening relative to the parafoveal ONL and OS length, respectively. In grade 2 FH, all features of grade 1 are present except the presence of a foveal pit. Grade 3 FH consists of all features of grade 2 FH except the widening of the cone OS. Grade 4 FH represents all the features seen in grade 3 except there is no widening of the ONL at the fovea. Finally, an atypical form of FH also is described in which there is a shallower pit with disruption of the inner segment ellipsoid. It is adapted with permission from Thomas et al.[1] **H,** Original OCT scans demonstrating the different grades of FH. Grades 1 and 2 can be considered to show signs of photoreceptor specialization (PRS+); however, grades 3 and 4 do not show signs of photoreceptor specialization (PRS−). ELM = external limiting membrane; GCL = ganglion cell layer; INL = inner nuclear layer; IPL = inner plexiform layer; ISe = inner segment ellipsoid; NFL = nerve fiber layer; ONL = outer nuclear layer; OPL = outer plexiform layer; PRS = photoreceptor specialization; RNFL = retinal nerve fiber layer; RPE = retinal pigment epithelium.

from the research ethics committee (research ethics committee references: (1) 20/EM/0040, (2) 31499, (3) 10/H0406/74, (4) 12/EM/0261).

To perform genetic analysis, genomic DNA was extracted from saliva samples or peripheral blood samples, dependent on protocols at each specific site. DNA was extracted as per manufacturer guidelines. Targeted next-generation sequencing panels,[11,15,16] whole exome sequencing,[17] whole genome sequencing,[17,18] or Sanger sequencing[11,12,19,20] was then performed. Individuals with a genetic diagnosis (including those with missing heritability, i.e., just 1 pathogenic variant) in the appropriate clinical context were included. Details of genetic analysis protocols have been published.[11,15,18] Briefly, our next-generation sequencing analysis protocol consisted of variant calling using the GATK pipeline (https://gatk.broadinstitute.org/) and further annotation using ANNOVAR (http://www.annovar.openbioinformatics.org/).

Data Extraction from Literature Review

Data were extracted from the literature by 5 experienced clinicians to identify previous reports of cases and cohorts of individuals with a diagnosis and foveal OCT. Literature searches were carried out using the databases PubMed, Medline, and Scopus. We applied a filter to search published literature between January 2011 and March 2021. Grading of FH was introduced in 2011; thus, we did not include literature before this.

Search terms included "optical coherence tomography" or "foveal hypoplasia" plus the diagnosis in question (e.g., "albinism," "PAX6"). To broaden our search strategy, we also included search terms "aniridia," "infantile nystagmus," and the abbreviations for ocular albinism ("OA") and oculocutaneous albinism ("OCA"). Syndromic forms of albinism, Hermansky−Pudlak syndrome (HPS), Chediak Higashi syndrome, and Griscelli syndrome were also searched for. An overview for the literature search approach is shown in Figure S1 (available at www.aaojournal.org). Further details of the cohort extracted from the literature are shown in Table S2 (available at www.aaojournal.org).

In cases where a foveal tomogram was provided, but no formal comment of foveal morphology was made, an experienced clinician would interpret and grade the tomogram using the Leicester Grading System.[1] Basic demographic and clinical characteristics were also collected where available. Visual acuity scores or

Table 1. List of Genes Associated with Typical and Atypical Foveal Hypoplasia with Genes Reported in this Study Highlighted in Bold

Condition	Clinical Phenotype	Gene	Location	MIM Gene ID	Phenotype Title	MIM Phenotype ID	Inheritance
OCA	A clinically and genetically heterogeneous disorder. Characterized by pigmentation defects of the hair, skin, and eyes. FH, chiasmal misrouting, infantile nystagmus, iris transillumination defects, fundus hypopigmentation.	**TYR**	11q14.3	606933	OCA1	203100, 606952	AR
		OCA2	15q12-q13	611409	OCA2	203200	AR
		TYRP1	9p23	115501	OCA3	203290	AR
		SLC45A2	5p13.2	606202	OCA4	606574	AR
		SLC24A5	15q21.1	609802	OCA6	113750	AR
		LRMDA (C10orf11)	10q22.2-q22.3	614737	OCA7	615179	AR
OA	Shares the same clinical characteristics as OCA, but with pigmentation defects generally limited to the eyes.	**GPR143**	Xp22.2	300808	OA1	300500	XL
HPS	A syndromic form of albinism demonstrating the same clinical characteristics as OCA in addition to blood platelet dysfunction with prolonged bleeding.	**HPS1**	10q24.2	604982	HPS1	203300	AR
		AP3B1	5q14.1	603401	HPS2	608233	AR
		HPS3	3q24	606118	HPS3	614072	AR
		HPS4	22q12.1	606682	HPS4	614073	AR
		HPS5	11p15.1	607521	HPS5	614074	AR
		HPS6	10q24.32	607522	HPS6	614075	AR
		DTNBP1	6p22.3	607145	HPS7	614076	AR
		BLOC1S3	19q13.32	609762	HPS8	614077	AR
		BLOC1S6	15q21.1	604310	HPS9	614171	AR
		AP3D1	19p13.3	607246	HPS10	617050	AR
		BLOC1S5	6p24.3	607289	HPS11	619172	AR
CHS	A syndromic form of albinism demonstrating the same clinical characteristics of OCA in addition to immune deficiency and ability to bruise and bleed easily.	LYST	1q42.3	606897	CHS1	214500	AR
FHONDA	FH, chiasmal misrouting, infantile nystagmus, and anterior segment dysgenesis in some cases (minor association).	**SLC38A8**	16q23.3	615585	FHONDA, FVH2	609218	AR
Aniridia	A panocular condition that can cause corneal and lens abnormalities, iris abnormalities (aniridia), raised intraocular pressure, foveal hypoplasia, infantile nystagmus, and optic nerve abnormalities.	**PAX6**	11p13	607108	AN1, FVH1	106210, 136520	AD
FRMD7-related infantile nystagmus	Associated with idiopathic infantile nystagmus. Most commonly associated with normal foveal morphology. Rare association with FH.	**FRMD7**	Xq26.2	300628	NYS1	310700	XL
AHR-related FH and infantile nystagmus	A recently reported condition characterized by FH and infantile nystagmus (only 2 cases reported in the literature, from the same family).	**AHR**	7p21.1	600253	*	-	AR
Achromatopsia	Characterized by cone photoreceptor dysfunction, reduced vision, and infantile nystagmus. Known to be associated with atypical FH and inner segment ellipsoid disruption.	**CNGB3**	8q21.3	605080	ACHM3	262300	AR
		CNGA3	2q11.2	600053	ACHM2	216900	AR
		GNAT2	1p13.3	139340	ACHM4	613856	AR
		PDE6C	10q23.33	600827	ACHM5	613093	AR
		PDE6H	12p12.3	601190	ACHM6	610024	AR
		ATF6	1q23.3	616517	ACHM7	605537	AR

ACHM = achromatopsia; AD = autosomal dominant; AR = autosomal recessive; CHS = Chediak–Higashi syndrome; FH = foveal hypoplasia; FHONDA = foveal hypoplasia, optic nerve decussation defects and anterior segment dysgenesis; HPS = Hermansky–Pudlak syndrome; MIM = Mendelian Inheritance in Man; OA = ocular albinism; OCA = oculocutaneous albinism; XL = X-linked.

fractions were converted to logarithm of the minimum angle of resolution (logMAR).

Individuals reported in publications authored by a collaborator site were omitted from the "literature cases" to avoid repeated data. For the purpose of reporting results, data from study sites and the literature were combined unless otherwise specified.

Statistical Analysis

Statistical analysis was carried out using SPSS software (IBM Corp, released 2019, IBM SPSS Statistics for Windows, version 26.0; IBM Corp). An average of right and left VA measurements was calculated and used for statistical analysis. Normality testing of the VA distribution was carried out with the Shapiro−Wilk test.

The Kruskal−Wallis test was used to test for statistical differences between average VA measurements across different diagnostic groups and grades of FH and to assess for statistical differences in average VA among the albinism subgroups, OCA, OA, and HPS. To test whether cone PRS was affected (PRS+ vs. PRS−), we performed the Pearson chi-square test. This allowed us to investigate whether there was a difference in the proportion of cases with and without cone PRS (PRS+ vs. PRS−) based on the genotype. We performed a subanalysis (Pearson chi-square test) within the albinism group, dividing the cohort into OCA, OA, and HPS. Post hoc analysis was performed as previously described,[21] and we report the adjusted residuals (adjusted z-scores) with adjusted P values (Bonferroni correction) to control for a type 1 error. All analyses were considered statistically significant when a probability value of $P \leq 0.05$ was identified.

Results

Overview of the Cohort

This multicenter study identified a total of 907 suitable individuals with genotypic and phenotypic data from study sites (57.7%) and the literature (42.3%). The mean age of the cohort was 22.7 years (standard deviation, 16.7 years), with a higher proportion of male individuals (53.6%) than female individuals (46.4%). The age and gender breakdowns per diagnostic group are shown in Figure S2 (available at www.aaojournal.org). In the achromatopsia cohort (n = 310), atypical FH was observed in 67.4% of cases (Fig 2A). Among individuals with variants in genes linked to typical FH (n = 597), we observed typical FH in 81.6% (Fig 2A).

Comparison of VA among Typical Foveal Hypoplasia, Atypical Foveal Hypoplasia, and Normal Foveal Morphology

Atypical FH had a significantly worse VA ($P < 0.0001$) than the typical FH group and the normal foveal morphology group (Fig 3A). Further analysis with typical FH split into each grade of FH revealed significant ($P < 0.05$) differences in VA (Fig 3B) for all pairwise comparisons except between grade 2 and 3 FH.

Typical FH: Genetic Etiologies, Photoreceptor Specialization, and Visual Acuity

Genetic Etiologies. The breakdown of genetic etiologies of typical FH (n = 487) included albinism (67.5%), *PAX6*

variants (21.8%), *SLC38A8* variants (6.8%), *FRMD7* variants (3.5%), and *AHR* variants (0.4%) (Fig 2B). Grade 4 FH was the most frequently reported grade of FH in this study (43.1%), and grade 2 was the least prevalent (14.0%) (Fig 4). An overview of the spectrum of typical FH OCT tomograms associated with each diagnosis is shown in Figure 4. The genotypic spectrum for the cases of typical FH is shown in Table S3 (available at www.aaojournal.org).

Photoreceptor Specialization. There was a significant difference in the grade of FH (PRS+ vs. PRS−) between the genetic etiologies (chi-square = 60.4, $P < 0.0001$). All *SLC38A8* variants were PRS− cases (adjusted z-score = 4.0, $P = 0.003$). In contrast, all *FRMD7* variants were PRS+ (adjusted z-score = 6.3, $P < 0.0001$). Likewise, subanalysis for albinism showed a significant difference in the grade of FH (PRS+ vs. PRS−) between the albinism subtypes (chi-square = 31.4, $P < 0.0001$). Post hoc analysis showed that HPS (adjusted z-score = 2.7, $P = 0.0065$) and OA (adjusted z-score = 4.5, $P < 0.0001$) were associated with only PRS− cases; however, OCA had a spectrum of both PRS+ and PRS− cases (adjusted z-score = 5.6, $P < 0.0001$).

Visual Acuity. There was a significant difference in VA between genetic etiologies associated with typical FH (H(3) = 21.3, $P < 0.0001$) (Fig 5). Multiple comparisons revealed that this was due to significant differences in VA between *FRMD7* and albinism (median difference = 0.30 logMAR, $P = 0.003$), *PAX6* (median difference = 0.40 logMAR, $P = 0.0004$), and *SLC38A8* (median difference = 0.31 logMAR, $P = 0.004$) (Fig 5A). The *FRMD7* group demonstrated the best VA, and the poorest median VA was associated with *PAX6* variants. Likewise, there was a significant difference in VA between the albinism subtypes (H(2) = 21.8, $P < 0.0001$). Multiple comparisons revealed that this was due to significantly better VA in OCA compared with OA (median difference = 0.14 logMAR, $P = 0.008$) and HPS (median difference = 0.28 logMAR, $P = 0.006$) (Fig 5B). Subanalysis of data only from study sites (i.e., excluding cases from the literature) showed similar results for both cone PRS and VA with genetic etiology (Table S4, available at www.aaojournal.org).

Discussion

This multicenter observational study represents the largest cohort of patients with FH providing significant insight into retinal development and visual prognosis based on a molecular diagnosis. We identified that albinism and *PAX6* variants are associated with a wide spectrum of arrested retinal development (grade 1−4 FH). Within the albinism group, OA and HPS had higher grades of FH (grade 3 and 4 FH), whereas a spectrum of FH (grade 1−4 FH) was observed in OCA. A narrow spectrum of FH was identified in *SLC38A8* variants (grade 3 and 4 FH) and *FRMD7* variants (grade 1 FH). Only 2 patients with *AHR* variants were reported in the literature, both with grade 3 FH; thus, more data on *AHR* variants must be analyzed to determine any association with degree of arrested retinal development.
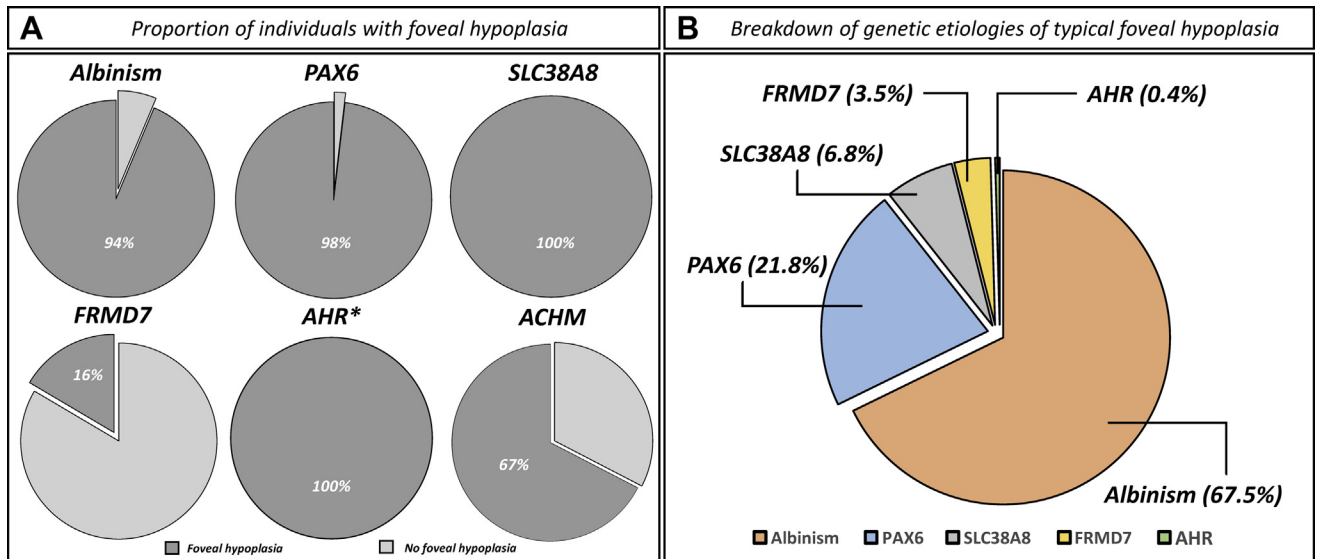
Figure 2. A, Proportion of individuals with foveal hypoplasia (FH) within each genetic diagnosis. **B,** Breakdown of genetic etiologies causative of typical FH. *Only 2 cases of AHR variants with FH were identified. ACHM = achromatopsia.

Consistent with the grade of FH, the *FRMD7* cohort had the best VA. Taken together, this highlights the central role of determining foveal morphology in patients because of its strong correlation to genetics and visual prognosis. Moreover, in scenarios where phenotypic data are lacking (e.g., an uncooperative patient), but the genotype is available, our data can guide clinicians in providing visual prognosis based on the correlations we describe in this study.[15,17]

There is a paucity of studies systematically comparing the different genetic etiologies associated with FH.[1,4] Previously, this has been limited to comparatively smaller cohorts or without a molecular diagnosis.[1,4] Consistent with previous studies characterizing foveal development in albinism or *PAX6* variants,[1,11,22] we highlight a spectrum of FH seen in both of these genetic conditions. This spectrum of FH is indicative of a variable timeframe of foveal developmental arrest in albinism and *PAX6* variants. On the contrary, *SLC38A8* and *AHR* variants

were consistently associated with high grades of FH (grades 3 and 4)[13,23]; thus, we hypothesize that arrested retinal development occurs at a more defined time period, earlier in development.[13] *FRMD7* variants were associated with grade 1 FH or normal foveal morphology,[24] therefore likely indicative of retinal developmental arrest at a later defined time point.

High grades of FH (grades 3 and 4) were consistently associated with OA and HPS. In contrast, OCA demonstrated a spectrum of FH (grade 1−4 FH). Genes involved in nonsyndromic OCA are generally enzymes or ion channels/exchangers.[25] Previous in vitro studies have shown that hypomorphic variants in *TYR* can exhibit reduced enzymatic activity of tyrosine hydroxylase and DOPA oxidase.[26] Thus, the FH spectrum seen in OCA could be due to the variable enzymatic function. In the presence of residual enzyme activity, partial pigmentation may be present as previously described in oculocutaneous
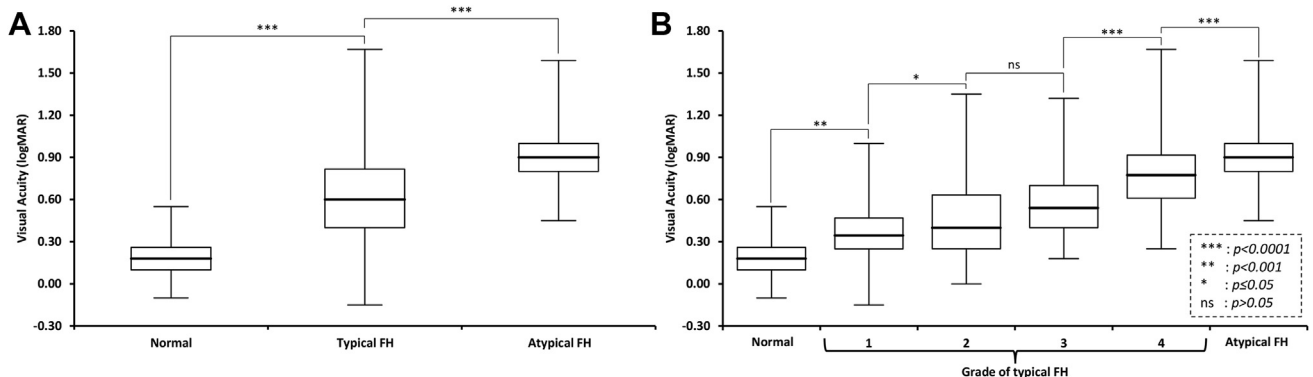
Figure 3. A, Box and whisker plots of visual acuity (VA) in individuals with normal foveal morphology compared with typical foveal hypoplasia (FH) and atypical FH. Pairwise comparisons show significant differences among the 3 groups. **B,** Pairwise comparisons with typical FH split into individual grades (1−4) show significant differences across all groups except between grades 2 and 3 FH.
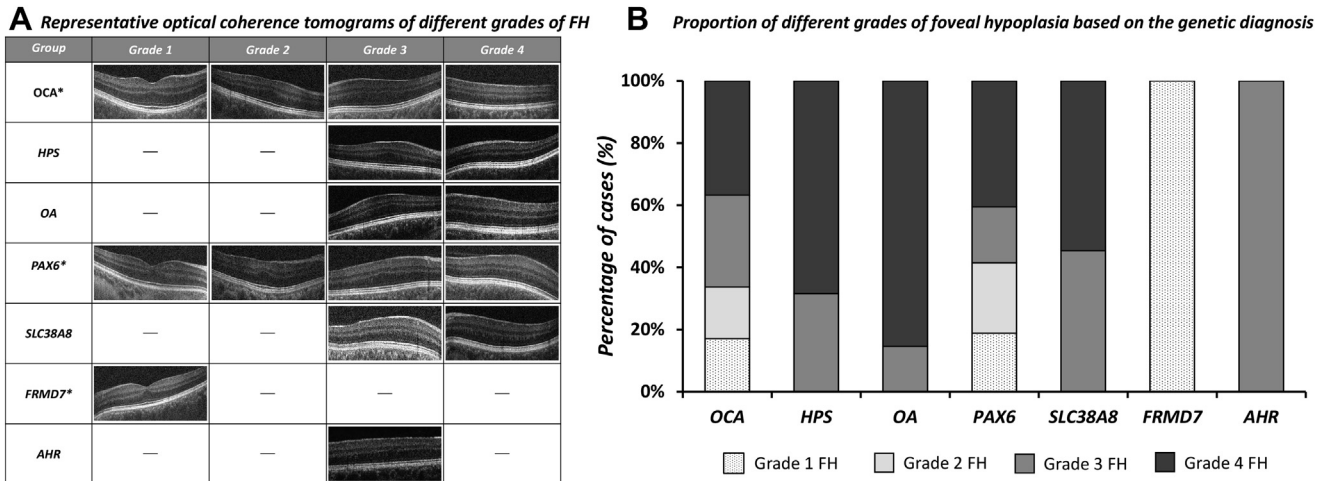
Figure 4. A, Representative tomograms of typical foveal hypoplasia (FH) in different genetic etiologies. **B,** The relative proportions of each grade of FH within each genetic diagnosis is shown in this bar chart. Nonsyndromic oculocutaneous albinism (OCA) and PAX6 variants had the full spectrum of FH; However, SLC38A8 variants, GPR143 variants associated with ocular albinism (OA), and variants associated with Hermansky−Pudlak syndrome (HPS) only had grade 3 and 4 FH. FRMD7 only had grade 1 FH. AHR only had grade 3 FH. *Albinism, PAX6, and FRMD7 can also have normal foveal morphology.

albinism type 1B (OCA1B) patients.[27] Conversely, HPS genes encode proteins that regulate intracellular vesicle trafficking, whereas OA is caused by variants in GPR143, which is an intracellular G-protein coupled receptor.[25] Both GPR143 and HPS genes are considered to be crucial for melanosome biogenesis. Previous in vitro studies show that deletions and nonsense GPR143 variants produce no protein or rapidly degraded truncated proteins. Likewise, the majority of GPR143 missense variants cause significant protein misfolding with an inability to exit the endoplasmic reticulum; thus, these variants are thought to have a similar pathogenesis to the large deletion and splice pathogenic variants.[28,29] We hypothesize that this cellular phenotype and impact on melanosome biogenesis translate to a more severe clinical phenotype with earlier arrested retinal development and worse visual prognosis.

The proportion of atypical FH in the achromatopsia group is similar to previous studies, with Thomas et al[30]

previously identifying 69% of achromatopsia individuals with atypical FH. Earlier work has shown that the foveal avascular zone is intact in achromatopsia.[31] This implies that normal cone photoreceptor development and function are important processes for structural development of the fovea. The outer retinal changes in achromatopsia can be progressive based on longitudinal studies[32]; however, further studies are needed to understand the relationship between cone photoreceptor dysfunction and foveal development.

We explored whether there was a difference in VA based on a molecular diagnosis. Albinism, SLC38A8, and PAX6 variants had similar median VAs (0.60−0.70 logMAR), whereas FRMD7 had significantly better median VA of 0.30 logMAR. FRMD7 variants were consistently associated with grade 1 FH or normal foveal morphology, thus demonstrating OS lengthening. Outer segment lengthening is a surrogate marker for peak foveal cone density.[5] Thus,
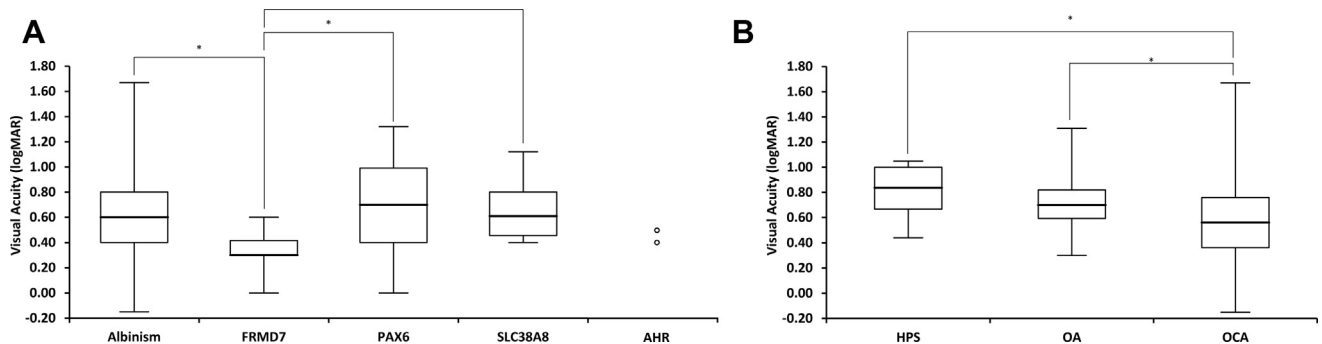

Figure 5. A, Box and whisker plots of visual acuity (VA) in each genetic etiology associated with foveal hypoplasia (FH). Only individuals with FH from each diagnostic group were included. **B,** Box and whisker plots of VA for albinism subtypes: nonsyndromic OCA, Hermansky−Pudlak syndrome (HPS), and ocular albinism (OA) due to GPR143 variants. The box represents the interquartile range. The line through the box represents the median, and the extent of whiskers represents the range. *Significant comparisons ($P \leq 0.05$). logMAR = logarithm of the minimum angle of resolution.

the OS lengthening in *FRMD7* indicates a more tightly packed cone photoreceptor mosaic with foveal specialization than other genetic etiologies, resulting in good visual prognosis. This is consistent with previous literature describing better median VA in *FRMD7* than albinism.[33] Albinism, *PAX6,* and *SLC38A8* had worse VA, which could be due to the predominantly higher grades of FH (grade 3 and 4 FH) observed. This represents a lack of OS lengthening (or PRS−).[13] Although the median VAs for albinism and *PAX6* group were 0.60 logMAR and 0.70 logMAR, respectively, a large distribution of VA was observed, thus reflecting the spectrum of FH grade (grades 1−4 FH) associated with both conditions. Furthermore, *PAX6* variants are associated with panocular phenotypes and significant phenotypic heterogeneity, thus likely providing a further explanation for the variance in VA.[4,34] In the achromatopsia group, individuals with atypical FH demonstrated worse VA than those with typical FH or normal foveal morphology. This is consistent with our previous reports and is likely due to the cone photoreceptor dysfunction.[1] The grade of FH has been recognized to facilitate the prediction of future VA in preverbal children.[1,7] Therefore, identifying the grade of FH provides significant prognostic value.[7]

Study Limitations

A limitation of our study was the exclusion of data from individuals without a molecular diagnosis but with a report of foveal morphology on OCT. Thus, individuals with deep intronic variants or novel variants may have been missed from our analysis. Likewise, data extracted from the literature represent a subset of patients who met the inclusion criteria and may not be representative of the entire cohorts reported within each study. Although every effort was made to record best-corrected VA, it is possible that, in PAX6, the presence of panocular phenotypes (e.g., cataracts and anterior segment dysgenesis) could be a contributing factor to the reduced VA, in addition to the presence of FH. Likewise, nystagmus can be variable between cases, and this could contribute to reduced VA. Furthermore, it is possible that our cohort has some selection bias because we included patients who had FH as determined by an OCT, thus potentially excluding patients with media opacities, such as cataracts and associated keratopathy. The inclusion of data obtained before the introduction of the Leicester Grading System in 2011 posed a challenge because of the inconsistency with

reported degree of arrested retinal development due to the lack of consensus on a suitable grading system for foveal underdevelopment.[1,35−38] Moreover, most reports before 2011 used time-domain OCT with limited spatial resolution for sufficient FH grading. We only included data from 2011 onward to ensure the standardized grading of FH by using the same classification system across all disorders.[1] Wilk et al[39] proposed the subdivision of grade 1 FH into grade 1a (extrusion of plexiform layers but with a nearly normal pit) and 1b (extrusion of plexiform layers with a shallow pit), which has since been included as part of the Leicester Grading System[7]; however, because of its recent introduction, many centers and subsequent publications are yet to adopt the new subclassification; therefore, we categorized the grade of FH only as grades 1 through 4 to maintain consistency with grading. Often in clinical environments, patients may be identified for analysis due to an obvious phenotype, for example, those demonstrating nystagmus. This may give rise to selection bias, where more severe grades of FH have been overrepresented in our cohort. Our study design included only qualitative reports of foveal morphology and genotype. Further studies to perform quantitative analysis across the retinal developmental disorders are required to investigate the potentially more subtle relationships with foveal morphology, function, and genotype. Furthermore, our study looked at genotype on a gene level only; therefore, future work investigating the genotype−phenotype relationships on a variant level is required.

In conclusion, this multicenter collaborative study has used the largest dataset so far to reveal genotypic correlations with foveal development and its consequence to vision. This provides mechanistic insight into how genes involved in foveal development interact at different temporal points resulting in varying degrees of arrested retinal development. Variants of *SLC38A8, GPR143, AHR,* and genes involved in HPS are associated with high grades of FH and poor cone PRS, which translates to earlier foveal developmental arrest and worse visual prognosis. This has significant diagnostic and prognostic value and can help with prioritization of genetic testing, subsequent counseling, and support.

Acknowledgments

Footnotes and Disclosures

[1] The University of Leicester Ulverscroft Eye Unit, Department of Neuroscience, Psychology and Behaviour, University of Leicester, Leicester, United Kingdom.

[2] Academic Unit of Ophthalmology and Orthoptics, University of Sheffield, Sheffield, United Kingdom.

[3] Institute of Vision Research, Department of Ophthalmology, Gangnam Severance Hospital, Yonsei University College of Medicine, Seoul, Korea.

[4] Department of Ophthalmology, Rigshospitalet, Denmark.

[5] Department of Clinical Medicine, University of Copenhagen, Copenhagen, Denmark.

[6] Department of Ophthalmology, University Medical Centre Utrecht, Utrecht, The Netherlands.

[7] Bartiméus Diagnostic Centre for Complex Visual Disorders, Zeist, The Netherlands.

[8] Department of Ophthalmology, The Rebecca D. Considine Research Institute and The Children's Vision Center, Akron Children's Hospital, Akron, Ohio; Department of Surgery, The Northeastern Ohio Medical University, Rootstown, Ohio.

[9] Department of Clinical Genetics, Rigshospitalet-Kennedy Center, Glostrup, Denmark.

[10] Department of Ophthalmology, Beijing Children's Hospital, National Center for Children's Health, Capital Medical University, Beijing, China.

[11] Department of Dermatology, Beijing Tongren Hospital, Capital Medical University, Beijing, China.

[12] Beijing Key Laboratory for Genetics of Birth Defects, Beijing Pediatric Research Institute; Rare Disease Center, National Center for Children's Health; MOE Key Laboratory of Major Diseases in Children, Beijing Children's Hospital, Capital Medical University, Beijing, China.

[13] Beijing Tongren Eye Centre, Beijing Tongren Hospital, Capital Medical University, Beijing Ophthalmology and Visual Science Key Lab, Beijing, China.

[14] Sorbonne Université, Institut National de la Santé et de la Recherche Médicale, Centre National de la Recherche Scientifique, Institut de la Vision, Paris, France; Exploration de la Vision et Neuro-Ophtalmologie, CHU de Lille, Lille, France.

[15] Department of Neurology, Pusan National University School of Medicine, Research Institute for Convergence of Biomedical Science and Technology, Pusan National University Yangsan Hospital, Yangsan, South Korea.

[16] Department of Health Sciences, University of Leicester, Leicester, United Kingdom.

[17] Department of Ophthalmology and Visual Neurosciences, University of Minnesota, Minneapolis, Minnesota.

[18] Centre for Ophthalmology and Visual Science (incorporating Lions Eye Institute), The University of Western Australia, Crawley, Australia.

[19] Retina and Vitreous Sector of Santa Casa de Misericórdia de São Paulo, São Paulo, Brazil.

[20] Sidney Kimmel Medical College of Thomas Jefferson University, Nemours Children's Health, Philadelphia, Pennsylvania.

[21] Ophthalmic Genetics and Visual Function Branch, National Eye Institute, National Institutes of Health, Bethesda, Maryland.

[22] Centre for Ophthalmology, Institute for Ophthalmic Research, University Tübingen, Tübingen, Germany.

[23] Rare Diseases, Genetics and Metabolism, INSERM U1211, University of Bordeaux, Bordeaux, France; Molecular Genetics Laboratory, Bordeaux University Hospital, Bordeaux, France.

[24] National Centre for Biotechnology (CNB-CSIC) and CIBERER-ISCIII, Madrid, Spain.

[25] Departments of Neurology and Ophthalmology, Boston Children's Hospital and Harvard Medical School, Boston, Massachusetts.

[26] Howard Hughes Medical Institute, Chevy Chase, Maryland.

[27] International Institute of Information Technology, Hyderabad, India.

[28] Foveal Development Investigators Group.

[29] Cooper Neurological Institute, Cooper Medical School of Rowan University, Camden, New Jersey.

[30] Nemours Children's Health, Wilmington, Delaware.

Abbreviations and Acronyms:

FH = foveal hypoplasia; **HPS** = Hermansky−Pudlak syndrome; **logMAR** = logarithm of the minimum angle of resolution; **OA** = ocular albinism; **ONL** = outer nuclear layer; **OS** = outer segment; **PRS** = photoreceptor specialization; **VA** = visual acuity.

Correspondence:

Mervyn G. Thomas, PhD, FRCOphth, University of Leicester Ulverscroft Eye Unit, Department of Neuroscience, Psychology and Behaviour, University of Leicester, RKCSB, LRI Leicester, United Kingdom LE2 7LX UK. E-mail: mt350@le.ac.uk.

References

1. Thomas MG, Kumar A, Mohammad S, et al. Structural grading of foveal hypoplasia using spectral-domain optical coherence tomography a predictor of visual acuity? *Ophthalmology*. 2011;118:1653−1660.
2. Hendrickson A, Possin D, Vajzovic L, Toth CA. Histologic development of the human fovea from midgestation to maturity. *Am J Ophthalmol*. 2012;154:767−778 e762.
3. Hendrickson AE, Yuodelis C. The morphological development of the human fovea. *Ophthalmology*. 1984;91:603−612.
4. Thomas MG, Papageorgiou E, Kuht HJ, Gottlob I. Normal and abnormal foveal development. *Br J Ophthalmol*. 2020 Nov 4; bjophthalmol-2020-316348. https://doi.org/10.1136/bjophthalmol-2020-316348. Online ahead of print.
5. Wilk MA, Wilk BM, Langlo CS, et al. Evaluating outer segment length as a surrogate measure of peak foveal cone density. *Vision Res*. 2017;130:57−66.
6. Springer AD, Hendrickson AE. Development of the primate area of high acuity. 1. Use of finite element analysis models to identify mechanical variables affecting pit formation. *Vis Neurosci*. 2004;21:53−62.
7. Rufai SR, Thomas MG, Purohit R, et al. Can structural grading of foveal hypoplasia predict future vision in infantile nystagmus? A longitudinal study. *Ophthalmology*. 2020;127:492−500.
8. Fujimoto J, Swanson E. The development, commercialization, and impact of optical coherence tomography. *Invest Ophthalmol Vis Sci*. 2016;57:OCT1−OCT13.
9. Huang D, Swanson EA, Lin CP, et al. Optical coherence tomography. *Science*. 1991;254:1178−1181.
10. Lee H, Purohit R, Patel A, et al. In vivo foveal development using optical coherence tomography. *Invest Ophthalmol Vis Sci*. 2015;56:4537−4545.
11. Kruijt CC, de Wit GC, Bergen AA, et al. The phenotypic spectrum of albinism. *Ophthalmology*. 2018;125:1953−1960.
12. McCafferty BK, Wilk MA, McAllister JT, et al. Clinical insights into foveal morphology in albinism. *J Pediatr Ophthalmol Strabismus*. 2015;52:167−172.
13. Kuht HJ, Han J, Maconachie GD, et al. SLC38A8 mutations result in arrested retinal development with loss of cone photoreceptor specialization. *Hum Mol Genet*. 2020;29:2989−3002.
14. Hvid K, Nissen KR, Bayat A, et al. Prevalence and causes of infantile nystagmus in a large population-based Danish cohort. *Acta Ophthalmol*. 2020 Feb 17. https://doi.org/10.1111/aos.14354. Online ahead of print.
15. Thomas MG, Maconachie G, Sheth V, et al. Development and clinical utility of a novel diagnostic nystagmus gene panel using targeted next-generation sequencing. *Eur J Hum Genet*. 2017;25:725−734.
16. Wei A, Yuan Y, Bai D, et al. NGS-based 100-gene panel of hypopigmentation identifies mutations in Chinese Hermansky-Pudlak syndrome patients. *Pigment Cell Melanoma Res*. 2016;29:702−706.
17. Rim JH, Lee ST, Gee HY, et al. Accuracy of next-generation sequencing for molecular diagnosis in patients with infantile nystagmus syndrome. *JAMA Ophthalmol*. 2017;135:1376−1385.
18. Gronskov K, Jespersgaard C, Bruun GH, et al. A pathogenic haplotype, common in Europeans, causes autosomal recessive albinism and uncovers missing heritability in OCA1. *Sci Rep*. 2019;9:645.
19. Thomas MG, Crosier M, Lindsay S, et al. The clinical and molecular genetic features of idiopathic infantile periodic alternating nystagmus. *Brain*. 2011;134:892−902.
20. Thomas S, Thomas MG, Andrews C, et al. Autosomal-dominant nystagmus, foveal hypoplasia and presenile cataract associated with a novel PAX6 mutation. *Eur J Hum Genet*. 2014;22:344−349.
21. Beasley T, Schumacker RE. Multiple regression approach to analyzing contingency tables: post hoc and planned comparison procedures. *Int J Exp Educ*. 1995;64:79−93.
22. Sannan NS, Gregory-Evans CY, Lyons CJ, et al. Correlation of novel PAX6 gene abnormalities in aniridia and clinical presentation. *Can J Ophthalmol*. 2017;52:570−577.
23. Mayer AK, Mahajnah M, Thomas MG, et al. Homozygous stop mutation in AHR causes autosomal recessive foveal hypoplasia and infantile nystagmus. *Brain*. 2019;142:1528−1534.
24. Thomas MG, Crosier M, Lindsay S, et al. Abnormal retinal development associated with FRMD7 mutations. *Hum Mol Genet*. 2014;23:4086−4093.
25. Montoliu L, Marks MS. A new type of syndromic albinism associated with mutations in AP3D1. *Pigment Cell Melanoma Res*. 2017;30:5−7.
26. Chaki M, Sengupta M, Mondal M, et al. Molecular and functional studies of tyrosinase variants among Indian oculocutaneous albinism type 1 patients. *J Invest Dermatol*. 2011;131:260−262.
27. King RA, Witkop CJ. Detection of heterozygotes for tyrosinase-negative oculocutaneous albinism by hairbulb tyrosinase assay. *Am J Hum Genet*. 1977;29:164−168.
28. d'Addio M, Pizzigoni A, Gassi MT, et al. Defective intracellular transport and processing of OA1 is a major cause of ocular albinism type 1. *Hum Mol Genet*. 2000;9:3011−3018.
29. Shen B, Rosenberg B, Orlow SJ. Intracellular distribution and late endosomal effects of the ocular albinism type 1 gene product: consequences of disease-causing mutations and implications for melanosome biogenesis. *Traffic*. 2001;2:202−211.
30. Thomas MG, Kumar A, Kohl S, et al. High-resolution in vivo imaging in achromatopsia. *Ophthalmology*. 2011;118:882−887.
31. Linderman RE, Georgiou M, Woertz EN, et al. Preservation of the foveal avascular zone in achromatopsia despite the absence of a fully formed pit. *Invest Ophthalmol Vis Sci*. 2020;61:52.
32. Thomas MG, McLean RJ, Kohl S, et al. Early signs of longitudinal progressive cone photoreceptor degeneration in achromatopsia. *Br J Ophthalmol*. 2012;96:1232−1236.
33. Kumar A, Gottlob I, McLean RJ, et al. Clinical and oculomotor characteristics of albinism compared to FRMD7 associated infantile nystagmus. *Invest Ophthalmol Vis Sci*. 2011;52:2306−2313.
34. Hingorani M, Williamson KA, Moore AT, van Heyningen V. Detailed ophthalmologic evaluation of 43 individuals with PAX6 mutations. *Invest Ophthalmol Vis Sci*. 2009;50:2581−2590.
35. Chong GT, Farsiu S, Freedman SF, et al. Abnormal foveal morphology in ocular albinism imaged with spectral-domain optical coherence tomography. *Arch Ophthalmol*. 2009;127:37−44.

36. Marmor MF, Choi SS, Zawadzki RJ, Werner JS. Visual insignificance of the foveal pit: reassessment of foveal hypoplasia as fovea plana. *Arch Ophthalmol*. 2008;126:907–913.
37. Mietz H, Green WR, Wolff SM, Abundo GP. Foveal hypoplasia in complete oculocutaneous albinism. A histopathologic study. *Retina*. 1992;12:254–260.
38. Seo JH, Yu YS, Kim HK, et al. Correlation of visual acuity with foveal hypoplasia grading by optical coherence tomography in albinism. *Ophthalmology*. 2007;114:1547–1551.
39. Wilk MA, McAllister JT, Cooper RF, et al. Relationship between foveal cone specialization and pit morphology in albinism. *Invest Ophthalmol Vis Sci*. 2014;55:4186–4198.

Pictures & Perspectives
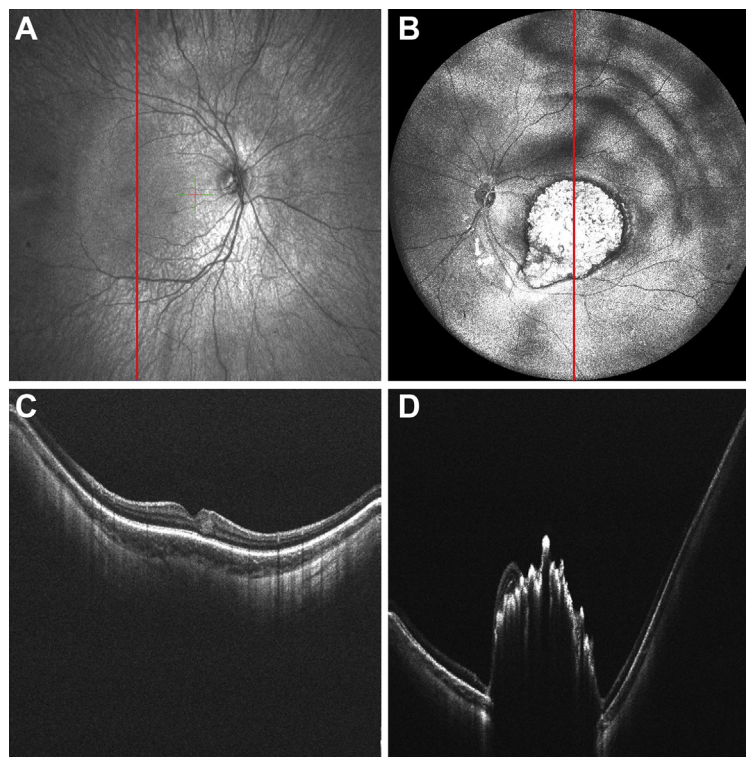
Ultrawide-field OCT for Retinoblastoma

Retinoblastoma tumors develop in young children, are often multifocal, large, and can occur anywhere in the retina. This has made the use of OCT in diagnosis and monitoring of retinoblastoma challenging. Using a prototype 400 kHz swept-source laser, we have developed an ultrawide-field handheld OCT system that permits evaluation of infants undergoing examination under anesthesia. We imaged both eyes of a 5-month-old patient with bilateral retinoblastoma who had completed 5 cycles of intravenous chemotherapy. Ultrawide-field OCT permits rapid, high-resolution imaging of both the smallest, subclinical tumors (Fig **A, C**) and large, elevated tumors (Fig **B, D**). (Magnified version of Fig **A-D** is available online at www.aaojournal.org).

ALISON H. SKALET, MD, PhD[1,2,3,4]
J. PETER CAMPBELL, MD, MPH[1]
YIFAN JIAN, PhD[1,5]

[1]Casey Eye Institute, Oregon Health & Science University, Portland, Oregon; [2]Knight Cancer Institute, Oregon Health & Science University, Portland, Oregon; [3]Department of Radiation Medicine, Oregon Health & Science University, Portland, Oregon; [4]Department of Dermatology, Oregon Health & Science University, Portland, Oregon; [5]Department of Biomedical Engineering, Oregon Health & Science University, Portland, Oregon

Footnotes and Financial Disclosures